Effect of Annealing and Hydrogen Radical Treatment on the Structure of Solution-Processed Hydrogenated Amorphous Silicon Films

Yoo Sakuma[1], Keisuke Ohdaira[1,2*], Takashi Masuda[1,3],

Hideyuki Takagishi[1,2], Zhongrong Shen[1,2], and Tatsuya Shimoda[1,2,3]

[1]Japan Advanced Institute of Science and Technology (JAIST)

1-1 Asahidai, Nomi, Ishikawa 923-1292, Japan

[2]JST-ALCA, Japan Science and Technology Agency (JST)

4-1-8 Honcho, Kawaguchi, Saitama 332-0012, Japan

[3]JST-ERATO, Japan Science and Technology Agency (JST)

*Tel: +81-761-51-1563, Fax: +81-761-51-1149, E-mail: ohdaira@jaist.ac.jp

Abstract

We investigate the structure distribution of solution-processed (Sol. P) hydrogenated amorphous silicon (a-Si:H) films along a thickness direction and the effect of hydrogen-radical treatment (H-treatment) by Raman spectroscopy. Sol. P a-Si:H films have a stress distribution along the thickness direction, and the degree of the distribution depends on annealing temperature and duration. H-treatment affects stress and short-range order (SRO) of a-Si:H films. These results give us a suggestion about the formation mechanism of Sol. P a-Si:H films through network reconstruction and H-treatment.

Keywords: amorphous silicon, solution process, stress, Raman

1. Introduction

Thin-film solar cells have advantages over bulk crystalline Si solar cells in ease of large area module production, more cost-effective manufacturing and a variety of applications [1]. In particular, hydrogenated amorphous silicon (a-Si:H) solar cells is an attractive candidate because a lot of efforts have been done in materials research, device physics, and process engineering [2-6]. But the reduction of fabrication cost is still not sufficient in views of the utilization of large-sized and costly apparatuses. The use of a solution process would solve this problem since it needs no expensive vacuum-based equipment [7, 8]. We have previously reported that a-Si:H films can be formed by spin-coating and annealing of "Si ink", consisting of polydihydrosilane (-$(SiH_2)_n$-) and organic solvent [9, 10]. We have so far fabricated superstrate-type solar cells by using p-type, intrinsic, and n-type a-Si:H films all formed by the solution process, and confirmed actual cell operation [11]. We have also reported the result of Raman spectroscopy in the entire solution-processed (Sol. P) a-Si:H films, and revealed that annealing at higher temperature leads to the formation of a-Si:H films with higher short-range order (SRO) [9]. In the formation of Sol. P a-Si:H films, large amount of gas molecules are released from the surfaces of the films during annealing [12]. This can lead to the formation of structural distribution along a thickness direction of the Sol. P a-Si:H films.

Hydrogen-radical treatment (H-treatment) to Sol. P a-Si:H films can improve their electrical property and solar cell performance [11]. One of the reasons for the improvement in the electrical property of Sol. P a-Si:H films by the H-treatment is a significant decrease in dangling bond density, evaluated by electron spin resonance (ESR), from 5×10^{17} to less than 2×10^{16} cm^{-3} [12]. It is expected that the H-treatment might also affect the structure of Sol. P a-Si:H films.

In this study, we evaluate the structure distribution of Sol. P a-Si:H films along a thickness direction by Raman spectroscopy. We also investigate the effect of H-treatment on the vertical structural distribution of Sol. P a-Si:H films.

2. Experimental

We used Si ink consisting of cyclooctane, acting as solvent, and polydihydrosilane as precursor for a-Si:H. Polydihydrosilane was synthesized by the photo-induced ring-opening polymerization of cyclopentasilane (CPS: Si_5H_{10}) [13] employing the Kipping method [14, 15], and was dissolved in cyclooctane at a concentration of 20-25 wt.%. The molar mass of polydihydrosilane ranges broadly from 10^2 to 10^6 g/mol [13]. We produced a-Si:H films by spin-coating the Si ink onto quartz substrates and annealing them in a globe box, in which O_2 concentration and dew point were kept at less than 0.5 ppm and -75 °C, respectively. After annealing, the thickness of the a-Si:H films were 160-200 nm. Annealing temperature (T_p) and duration (t_p) strongly affect film property, and were thus systematically varied. For the investigation of T_p dependence, the a-Si:H samples were prepared by annealing at T_p = 360, 390, and 420 °C for a fixed annealing duration of t_p =15 min. In order to check the effect of high T_p, we carried out an additional annealing at 500 °C for 15 min on the a-Si:H sample prepared at T_p = 420 °C. We also investigated the influence of annealing duration on the Sol. P a-Si:H film structure. Annealing duration was varied from 20 sec to 30 min at a fixed T_p = 390 °C.

Next, we investigated the structural change of Sol. P a-Si:H films by H-treatment in a catalytic chemical vapor deposition (Cat-CVD) chamber. A tungsten wire with a diameter of 0.5 mm and a length of 100 cm was used as a catalyzer and heated at

1850 °C. Hydrogen gas (99.9999% purity) was introduced into the chamber at a flow rate of 16 sccm for 15 min. The chamber pressure and the substrate temperature during the H-treatment were maintained at 0.15 Pa and 220 °C, respectively.

Raman spectroscopy is a powerful tool to investigate network structure of a-Si:H [16-21]. We used three lasers in Raman spectroscopy: He-Cd laser (λ = 442 nm), Ar^+ laser (λ = 488 nm), and He-Ne laser (λ = 633 nm). He-Ne laser has a long penetration depth for a-Si:H (≈ 300 nm), and the results obtained by using this laser reflects the property of entire films. The other two lasers have much shorter penetration depth (≈ 30 nm), and surface-sensitive Raman spectra can be obtained. In order to measure the internal structure of films by lasers with short penetration depth, we repeated reactive ion etching (RIE) using Ar gas. This approach can reveal more precise structural distribution of a-Si:H films than that reported previously by Morell *et al.*, using lasers with different penetration depths [22].

In the Raman spectra of the Sol. P a-Si:H films, a transverse optical (TO) peak, whose peak position is around 470-480 cm^{-1}, is an important parameter to evaluate SRO and film stress. The full width at half maximum (FWHM) of TO (Γ_{TO}) is related with SRO [23-25]. TO peak position (ω_{TO}) is associated with stress [26, 27]. In order to obtain Γ_{TO} and ω_{TO} accurately, the Raman data was fitted to a Gaussian function.

3. Results and Discussion

3.1. Annealing temperature dependence

Figure 1 shows the Ar^+ laser Raman spectra of Sol. P a-Si:H films prepared at T_p = 390 °C for t_p =15 min. TO peak monotonically shifts to higher by repeating RIE and reducing film thickness. This means that ω_{TO} is smaller near the surface than near the

bottom. Figures 2(a) and (b) show the ω_{TO} and Γ_{TO} in various T_p as a function of remaining film thickness, respectively. All the samples shown in this figure were annealed for 15 min and measured with Ar^+ laser. One can see clear tendency of ω_{TO} increasing from the surface to the bottom of the films in all the samples. It is also confirmed that, at higher T_p, not only the value of ω_{TO} but also the gradient of ω_{TO} from surface to bottom region become smaller, and ω_{TO} reaches a constant value at high T_p. On the other hand, we can see no clear tendency of Γ_{TO} against remaining film thickness, as shown in Fig. 2 (b). Tsu found that not only Γ_{TO} but also ω_{TO} is associated with SRO [28]. But their result does not conflict with the case of ref. 27 and the Sol. P a-Si:H films, which are formed under different fabrication condition.

These facts mean that there is no significant difference in SRO between the surface and bottom region, while the vertical distribution of tensile stress exists. The stress distribution is probably because of gas release from the surface of Sol. P a-Si:H films during annealing. At low T_p, gas release occurs more severely near the surface region, resulting in the larger gradient of tensile stress along the thickness direction. On the contrary, large amount of gas molecules are released also from the interior of the Sol. P a-Si:H films at high T_p. This leads to the generation of large and relatively uniform tensile stress through the entire a-Si:H films, resulting in less stress distribution along a thickness direction.

Figure 3 shows the Raman spectra of the Sol. P a-Si:H films prepared at T_p = 390 °C for t_p = 15 min, measured with He-Cd and He-Ne lasers. These spectra exhibit the properties of the surface region and the entire film, respectively. As mentioned above, ω_{TO} near the film surface is smaller than that in the entire film, which is consistent with the result shown in Fig. 2(a). Γ_{TO} in the entire film is larger than the film

surface. This is probably because of the significant ω_{TO} distribution along a thickness direction and resulting apparent broadening of the spectrum.

3.2. Annealing duration dependence

Figure 4 shows the He-Ne laser Raman spectra of the Sol. P a-Si:H films prepared at T_p = 390 °C for t_p varied from 20 sec to 30 min. At t_p = 20 sec and 1 min, the Raman spectra are far different from that of a-Si:H, indicating that the films are not fully converted to a-Si:H. Γ_{TO} dramatically decreases and ω_{TO} shifts to smaller wavenumber for longer t_p, which means that the SRO of films is significantly improved, and the a-Si:H films have larger tensile stress at longer t_p. Figures 5 show the ω_{TO} for various t_p as a function of remaining thickness. We employed He-Cd laser for this measurement. ω_{TO} tends to be lower near the surface and higher near the substrate. For longer t_p, the value of ω_{TO} becomes small, and reaches a constant value. The gradient of ω_{TO} along a thickness direction becomes largest at t_p = 4 min. The tendency of ω_{TO} variation can be considered as an increase in tensile stress due to enhanced gas release for longer t_p, similar to the effect of increased T_p. For t_p < 1 min, a-Si:H network is not formed sufficiently, and no significant tensile stress exists. At $t_p \approx$ 4 min, a-Si:H is formed along with gas release, and the gradient of tensile stress becomes large. For longer t_p, large amount of gas molecules are released also from interior of films, resulting in larger tensile stress and smaller stress distribution along thickness direction.

3.3. Effect of H-treatment

Figures 6(a) and (b) show the He-Cd laser Raman spectra of the Sol. P a-Si:H films prepared at T_p = 390 °C for t_p = 15 min before and after H-treatment. We can see a clear peak shift to higher ω_{TO} and a reduction in Γ_{TO} after H-treatment on the surface of the Sol. P a-Si:H film in Fig. 6(a). These are indications of improvement in the SRO and a

reduction in the tensile stress of the surface of the Sol. P a-Si:H film by H-treatment. Two peaks at around 2000 cm^{-1} and 2090 cm^{-1} are seen in Fig. 6(b). In general, the former peak is identified as monohydride (Si-H) configuration, and the latter is of dihydride ($Si-H_2$) configuration or hydride near voids, respectively [29, 30]. It can be seen that a monohydride peak increases by H-treatment, while no significant change occurs in a dihydride peak. One possible explanation of these phenomena is the incorporation of H atoms into tensilely-stressed Si-Si bonds and the formation of additional Si-H bonds. Of course, dangling bonds in the Sol. P a-Si:H films are terminated by H, and Si-H bonds are also be newly created. The density of dangling bonds (5×10^{17} cm^{-3}) [11] is, however, much far from a detectable level in our Raman spectroscopy system, and the termination of dangling bonds cannot be the primary reason of the increase in a Si-H signal shown in Fig. 6(b). It should be noted that the $Si-H_2$/Si-H peak ratio obtained by the Raman spectroscopy in this study is significantly different from that of a Fourier-transform infrared (FT-IR) spectrum reported previously [9]. At present, we have no proper explanation for the difference. This might be related to the different sensitivities of the two peaks depending on the measurement method.

Figures 7(a) and (b) show the ω_{TO} in the Raman spectra of the Sol. P a-Si:H films prepared at various T_p before and after H-treatment as a function of remaining film thickness. H-treatment decreases the gradients of ω_{TO} along thickness direction which exists in the Sol. P a-Si:H before H-treatment. This probably means that H-treatment is more effective on the surface region, and a decrease in tensile stress by H introduction occurs selectively near the surface of the Sol. P a-Si:H films. Figure 8 shows the Γ_{TO} in the Raman spectra of the Sol. P a-Si:H films prepared at various T_p before and after H-treatment as a function of remaining film thickness. Small distribution of Γ_{TO} along

the thickness direction can be seen for the Sol. P a-Si:H films before H-treatment, while there is considerable Γ_{TO} distribution after H-treatment. This phenomenon is consistent with the previous consideration, that is, more incorporation of H atoms near the surface of the Sol. P a-Si:H films. Si-Si bonds with high tensile stress may be reconstructed to Si-H bonds by H incorporation, and as a result, the SRO of Si network is improved and Γ_{TO} decreases more effectively near the surface.

Figure 9(a) and (b) show the Raman spectra of the Sol. P a-Si film before and after H-treatment, which are to observe Si-H stretching modes. No remarkable difference is seen in the spectra for the Sol. P a-Si:H before H-treatment independent of remaining film thickness. After H-treatment, a Si-H peak clearly increases in the Raman spectrum measured near the surface, while the intensity of Si-H peaks is unchanged in the spectra measured at deeper parts. These results fully support our consideration about the variation of ω_{TO} and Γ_{TO} by H-treatment. Similar H distribution has also been reported previously from our group [31].

4. Conclusions

We have confirmed the existence of stress distribution in Sol. P a-Si:H films along the thickness direction. The stress distribution can be consistently understood as a gas release from the film surface. The idea of stress dependence on T_p and t_p give us a suggestion of the formation mechanism of a Sol. P a-Si:H film: outgassing and Si network reconstruction are critical for the film formation. We have also found that H-treatment affects to reduce tensile stress and to improve SRO particularly near the surface of Sol. P a-Si:H films as well as to decrease their defect density and to improve their electrical property.

Acknowledgement

This work is supported by JST ALCA program. And we would like to acknowledge Prof. M. Koyano for his help for Raman spectroscopy.

References

[1] S. Hegedus, Prog. Photovoltaics **14**, 393 (2006).

[2] B. Rech and H. Wagner, Appl. Phys. A **69**, 155 (1999).

[3] H. Sakai and Y. Ichikawa, J. Non-Cryst. Solids **137–138**, 1155 (1991).

[4] S. Guha, K. L. Narasimhan, and S. M. Pietruszko, J. Appl. Phys. **52**, 859 (1981).

[5] A. Banerjee and S. Guha, J. Appl. Phys. **69**, 1030 (1991).

[6] Y. Moriya, T. Krajangsang, P. Sichanugrist, and M. Konagai, Proc. 38th IEEE Photovoltaic Specialists Conf., 2012, p. 003020.

[7] J. Y. Kim, K. Lee, N. E. Coates, D. Moses, T.-Q. Nguyen, M. Dante, and A. J. Heeger, Science **317**, 222 (2007).

[8] W. Wang, Y.-W. Su, and C.-H. Chang, Sol. Energy Mater. Sol. Cells **95**, 2616 (2011).

[9] T. Masuda, Y. Matsuki, and T. Shimoda, Thin Solid Films **520**, 6603 (2012).

[10] T. Masuda, Y. Matsuki, and T. Shimoda, Thin Solid Films **520**, 5091 (2012).

[11] T. Masuda, N. Sotani, H. Hamada, Y. Matsuki, and T. Shimoda, Appl. Phys. Lett. **100**, 253908 (2012).

[12] T. Shimoda, Y. Matsuki, M. Furusawa, T. Aoki, I. Yudasaka, H. Tanaka, H. Iwasawa, D. Wang, M. Miyasaka, and Y. Takeuchi, Nature **440**, 783 (2006).

[13] T. Masuda, Y. Matsuki, and T. Shimoda, Polymer **53**, 2973 (2012).

[14] F. S. Kipping, J. Chem. Soc. **125**, 2291 (1924).

[15] E. Hengge and G. Bauer, Angew. Chem., Int. Ed. **12**, 316 (1973).

[16] R. Shuker and R. W. Gammon, Phys. Rev. Lett. **25**, 222 (1970).

[17] R. Tsu, J. Gonzalez-Hernandez, J. Doehler, and S. R. Ovshinsky, Solid State Commun. **46**, 79 (1983).

[18] T. D. Moustakas, T. Tiedje, and W. A. Lanford, AIP Conf. Proc. **73**, 20 (1981).

[19] S. T. Kshirsagar and J. S. Lannin, Phys. Rev. B **25**, 2916 (1982).

[20] T. Ishidate, K. Inoue, K. Tsuji, and S. Minomura, Solid State Commun. **42**, 197 (1982).

[21] E. Martínez and F. Ynduráin, Solid State Commun. **44**, 1477 (1982).

[22] G. Morell, R. S. Katiyar, S. Z. Weisz, H. Jia, J. Shinar, and I. Balberg, J. Appl. Phys. **78**, 5120 (1995).

[23] D. Beeman, R. Tsu, and M. F. Thorpe, Phys. Rev. B **32**, 874 (1985).

[24] R. Tsu, J. G. Hernandez, and F. H. Pollak, J. Non-Cryst. Solids **66**, 109 (1984).

[25] N. Maley, D. Beeman, and J. S. Lannin, Phys. Rev. B **38**, 10611 (1988).

[26] Y. Hishikawa, K. Watanabe, S. Tsuda, M. Ohnishi, and Y. Kuwano, Jpn. J. Appl. Phys. **24**, 385 (1985).

[27] Y. Hishikawa, J. Appl. Phys. **62**, 3150 (1987).

[28] R. Tsu, M. A. Paesler, and D. Sayers, J. Non-Cryst. Solids **114**, 199 (1989).

[29] M. H. Brodsky, M. Cardona, and J. J. Cuomo, Phys. Rev. B **16**, 3556 (1977).

[30] J. Shinar, H. Jia, R. Shinar, Y. Chen, and D. L. Williamson, Phys. Rev. B **50**, 7358 (1994).

[31] H. Murayama, T. Ohyama, I. Yoshida, A. Terakawa, T. Masuda, K. Ohdaira, and T. Shimoda, submitted to Thin Solid Films.

Figure captions

Fig. 1 Raman spectra of the Sol. P a-Si:H films prepared at T_p = 390 °C for t_p =15 min. The spectra were measured with Ar^+ laser. The values shown on left side of the data are remaining a-Si:H thickness after (or without) RIE.

Fig. 2 (a) ω_{TO} and (b) Γ_{TO} in the Raman spectra of the Sol. P a-Si:H films formed at various T_p as a function of remaining thickness.

Fig. 3 Raman spectra of the Sol. P a-Si:H films prepared at T_p = 390 °C for t_p = 15 min. The spectra were measured with He-Ne laser and He-Cd lasers.

Fig. 4 Raman spectra of the Sol. P a-Si:H films prepared at T_p = 390 °C for t_p = 20 sec to 30 min. The spectra were measured with He-Ne laser.

Fig. 5 ω_{TO} in the Raman spectra of the Sol. P a-Si:H films formed in various t_p as a function of remaining thickness.

Fig. 6 Raman spectra of the Sol. P a-Si:H films in the range of (a) 400-530 cm^{-1} and (b) 1900-2200 cm^{-1}. The Sol. P a-Si:H films were prepared at T_p = 390 °C for t_p =15 min. Both spectra are normalized with TO peak intensity. Broken and solid lines indicate the spectra of the a-Si:H film before and after H-treatment, respectively.

Fig. 7 ω_{TO} in the Raman spectra of the Sol. P a-Si:H films formed at various T_p (a) before and (b) after H-treatment as a function of remaining thickness.

Fig. 8 Γ_{TO} in the Raman spectra of the Sol. P a-Si:H films formed at various T_p (a) before and (b) after H-treatment as a function of remaining thickness.

Fig. 9 Raman spectra of the Sol. P a-Si:H films prepared at T_p = 420 °C for t_p =15 min (a) before and (b) after H-treatment. The spectra were measured with He-Cd laser. The values shown on right side of the data are remaining a-Si:H thickness after (or without) RIE. Both spectra are normalized with TO peak intensity.

Fig. 1

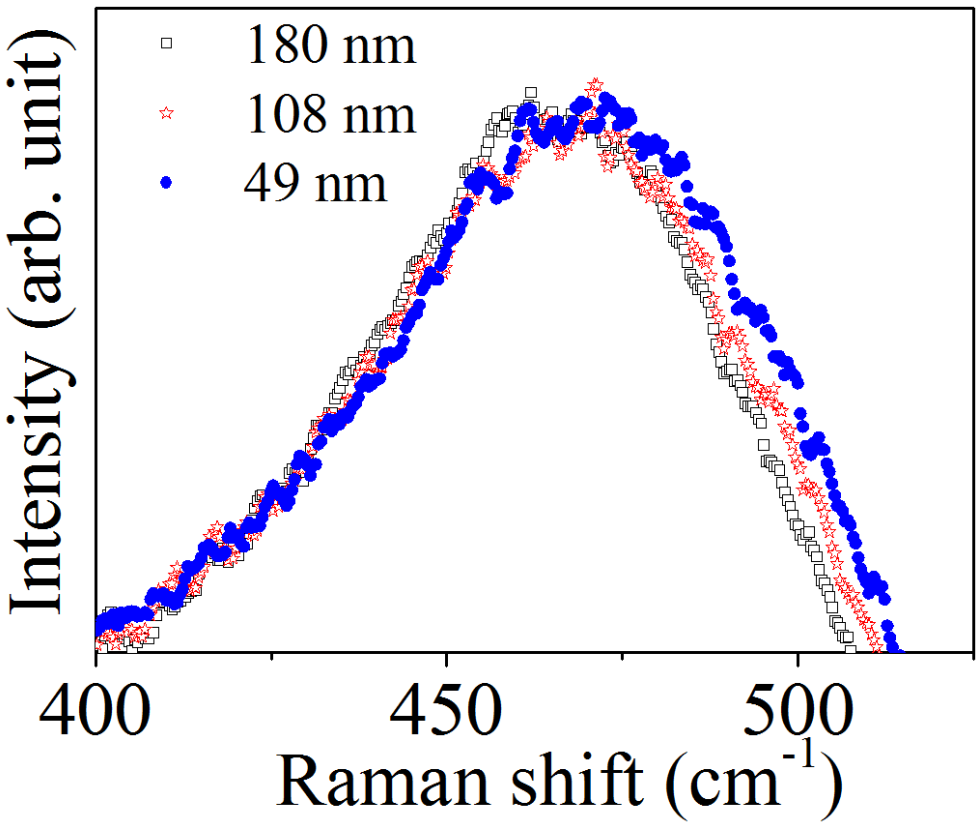
180 nm
108 nm
49 nm
Intensity (arb. unit)
400
450
500
Raman shift (cm-1)

Fig. 2

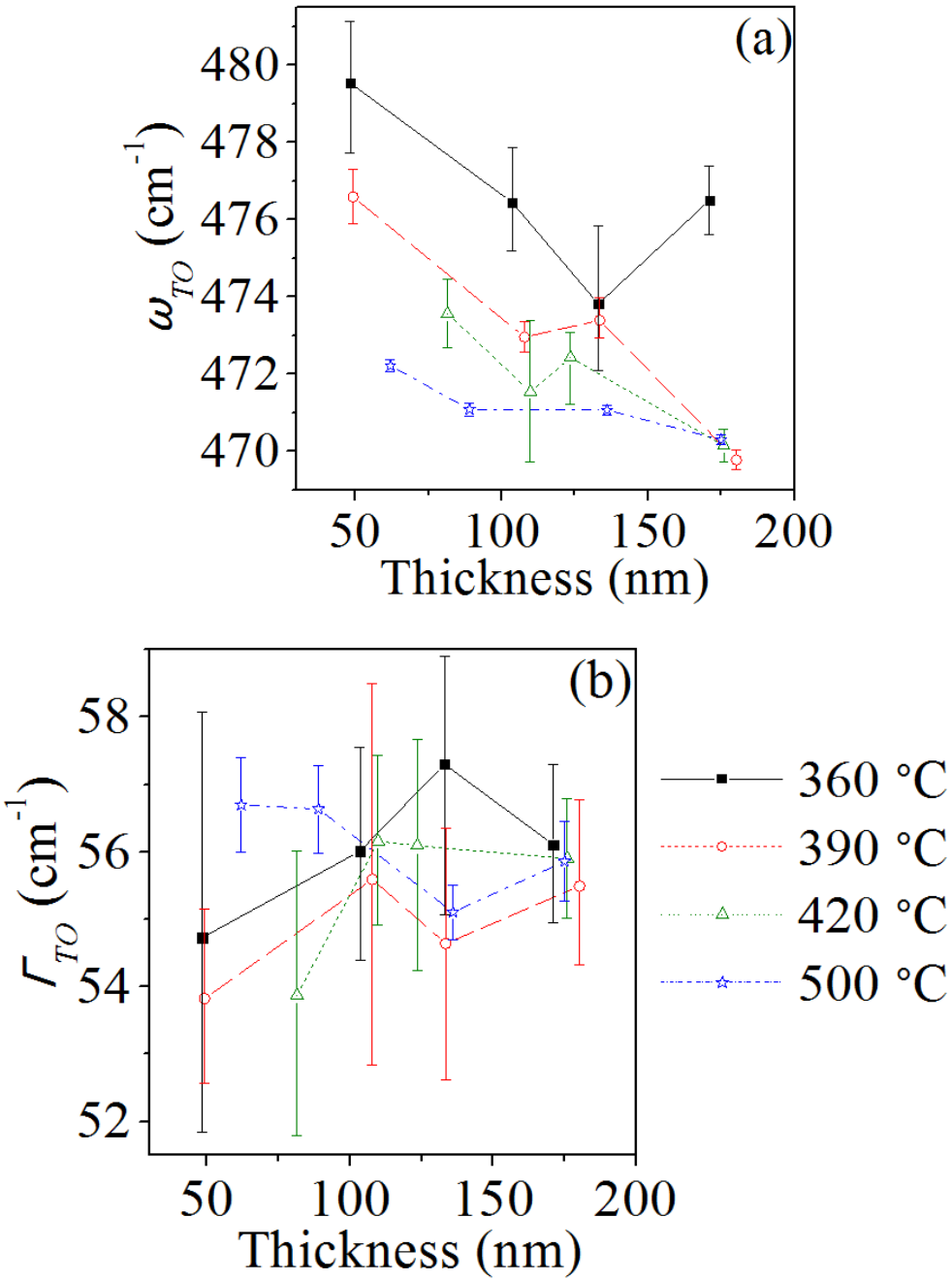
(a)
480
478
476
474
472
470
ω_{TO} (cm^{-1})
50
100
150
200
Thickness (nm)
(b)
58
56
54
52
Γ_{TO} (cm^{-1})
50
100
150
200
Thickness (nm)
360 °C
390 °C
420 °C
500 °C

Fig. 3

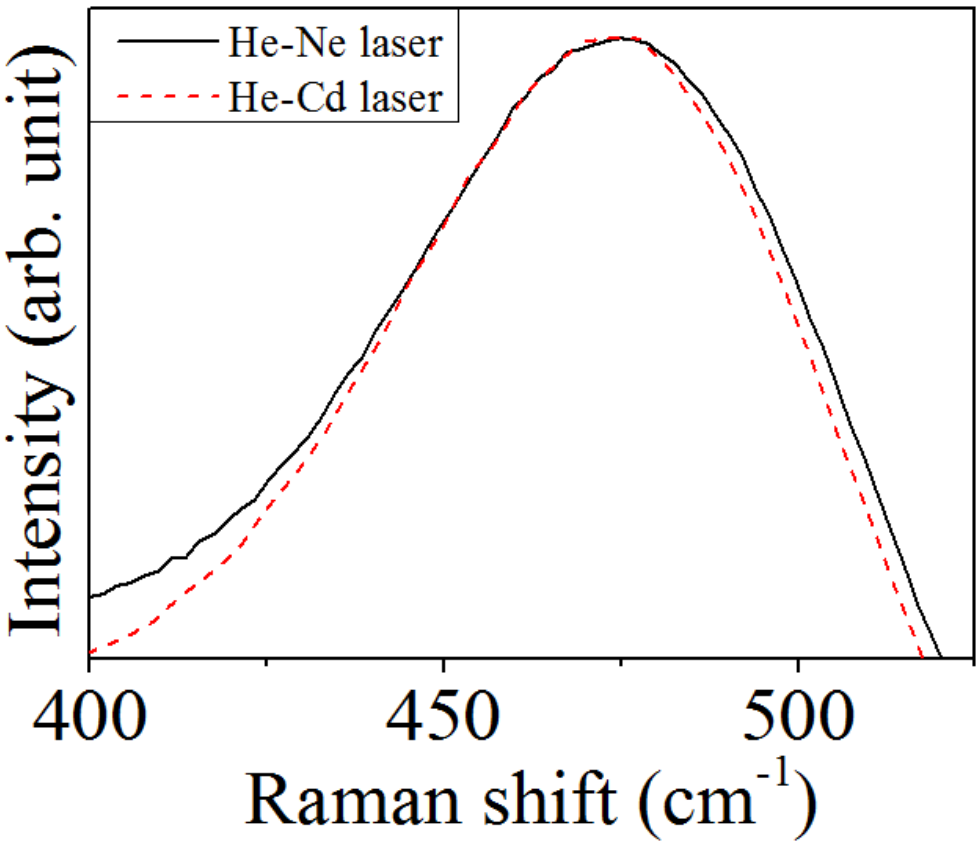
He-Ne laser
He-Cd laser
Intensity (arb. unit)
400
450
500
Raman shift (cm-1)

Fig. 4

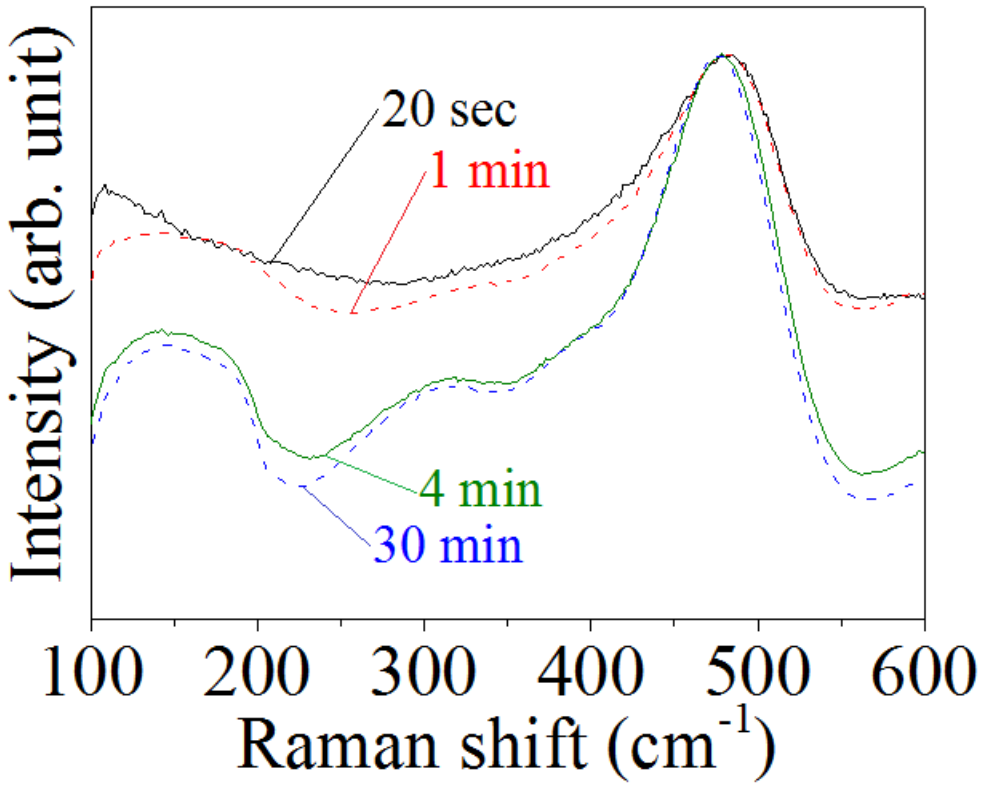
Intensity (arb. unit)
20 sec
1 min
4 min
30 min
100
200
300
400
500
600
Raman shift (cm-1)

Fig. 5

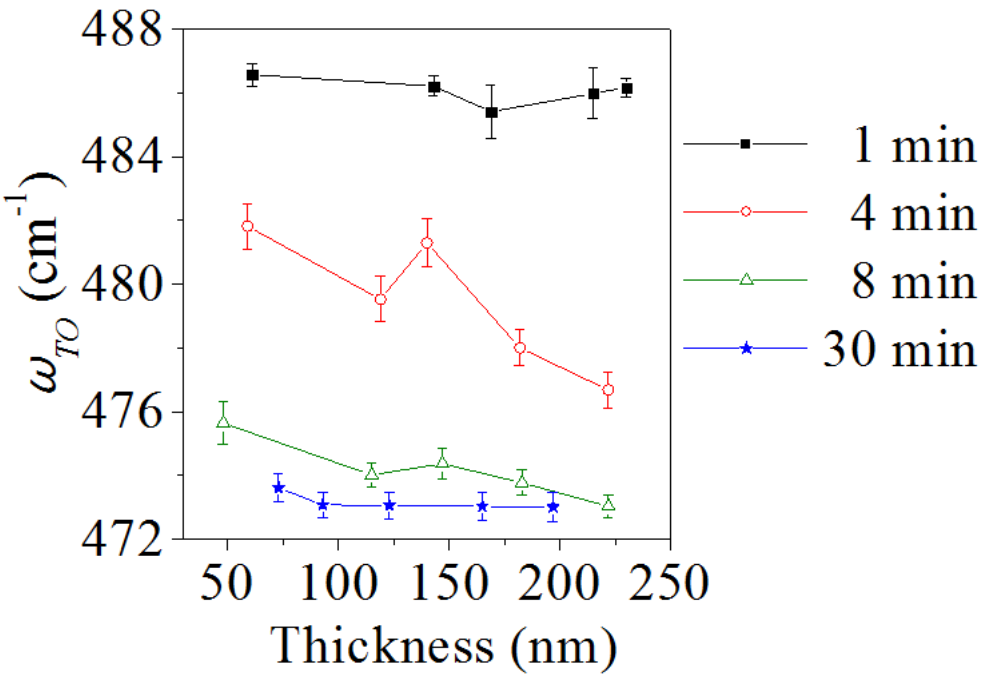
488
484
480
476
472
ω_{TO} (cm^{-1})
50
100
150
200
250
Thickness (nm)
1 min
4 min
8 min
30 min

Fig. 6

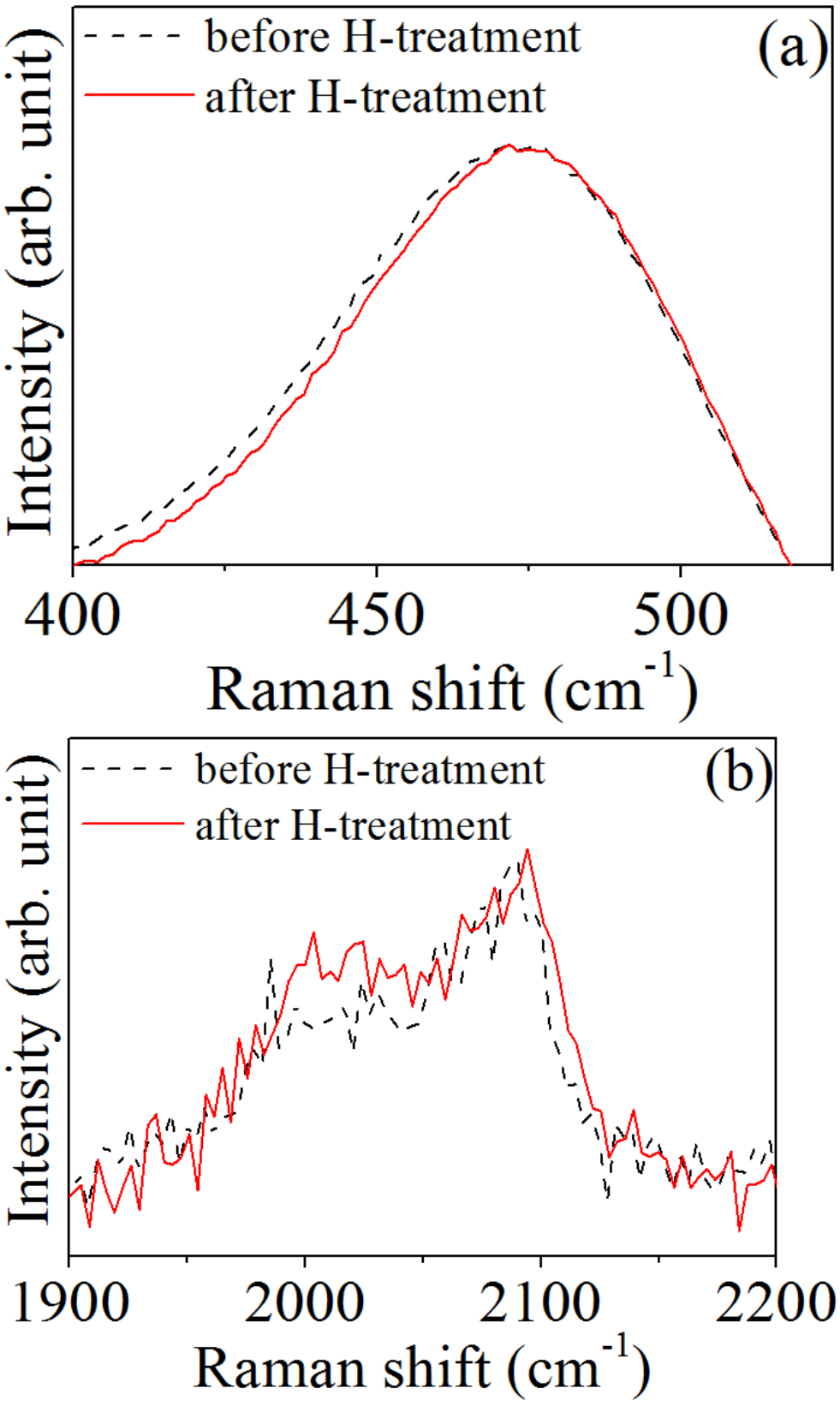
before H-treatment
after H-treatment
(a)
Intensity (arb. unit)
400
450
500
Raman shift (cm-1)
before H-treatment
after H-treatment
(b)
Intensity (arb. unit)
1900
2000
2100
2200
Raman shift (cm-1)

Fig. 7

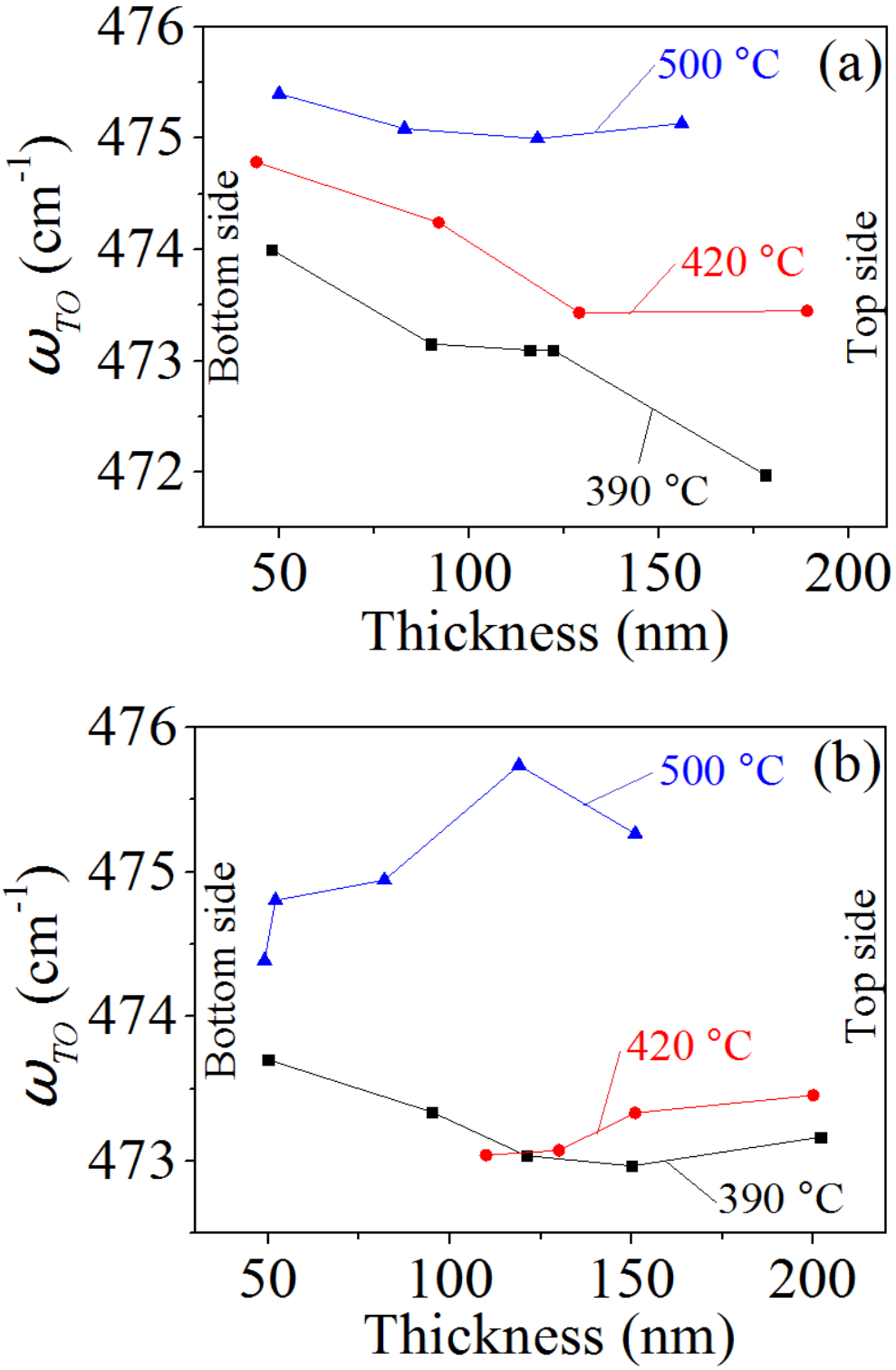
476
475
474
473
472
ω_{TO} (cm^{-1})
Bottom side
Top side
500 °C
420 °C
390 °C
(a)
50
100
150
200
Thickness (nm)
476
475
474
473
ω_{TO} (cm^{-1})
Bottom side
Top side
500 °C
420 °C
390 °C
(b)
50
100
150
200
Thickness (nm)

Fig. 8

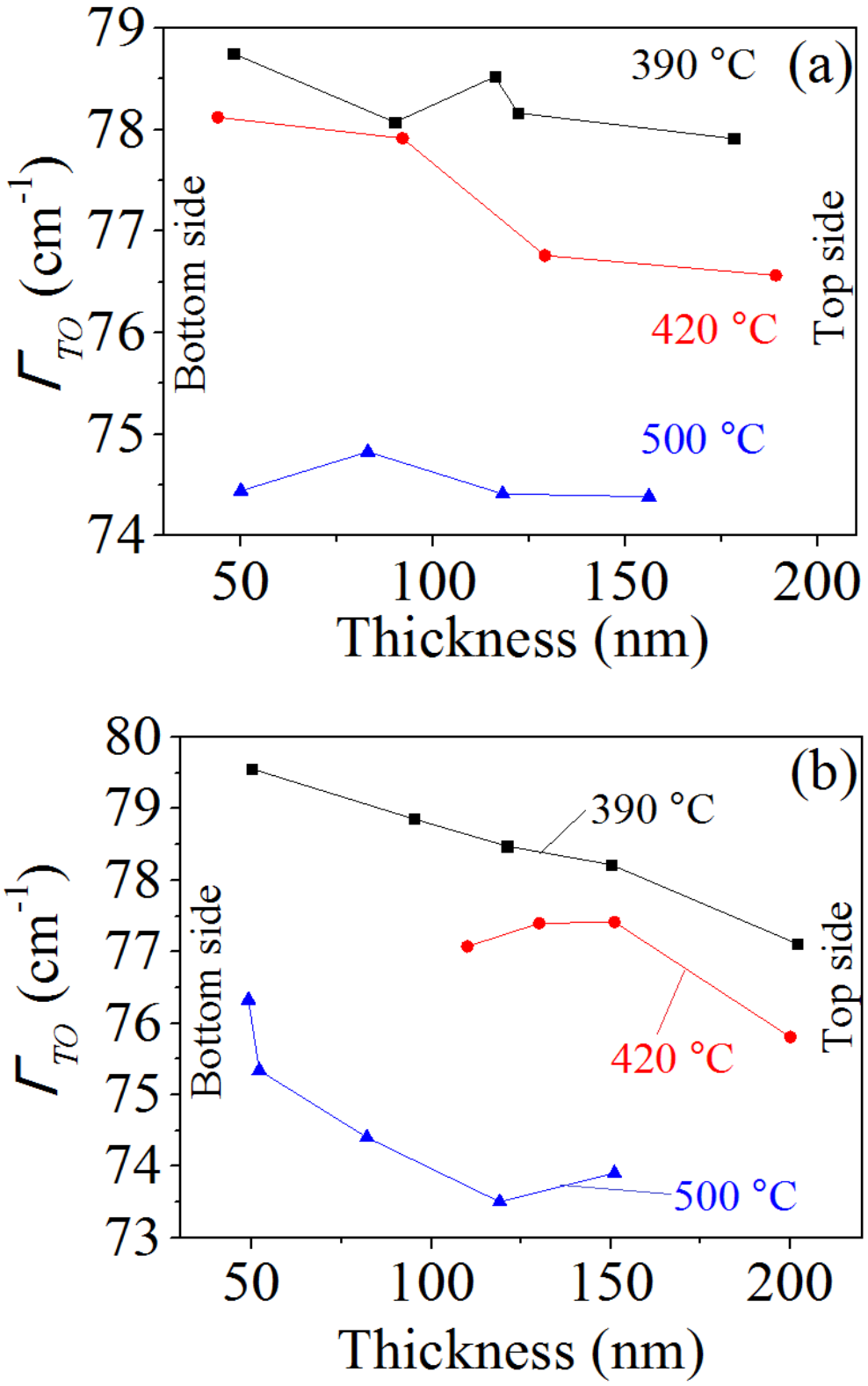
(a)
390 °C
420 °C
500 °C
Bottom side
Top side
Γ_{TO} (cm^{-1})
Thickness (nm)
79
78
77
76
75
74
50
100
150
200
(b)
390 °C
420 °C
500 °C
Bottom side
Top side
Γ_{TO} (cm^{-1})
Thickness (nm)
80
79
78
77
76
75
74
73
50
100
150
200

Fig. 9

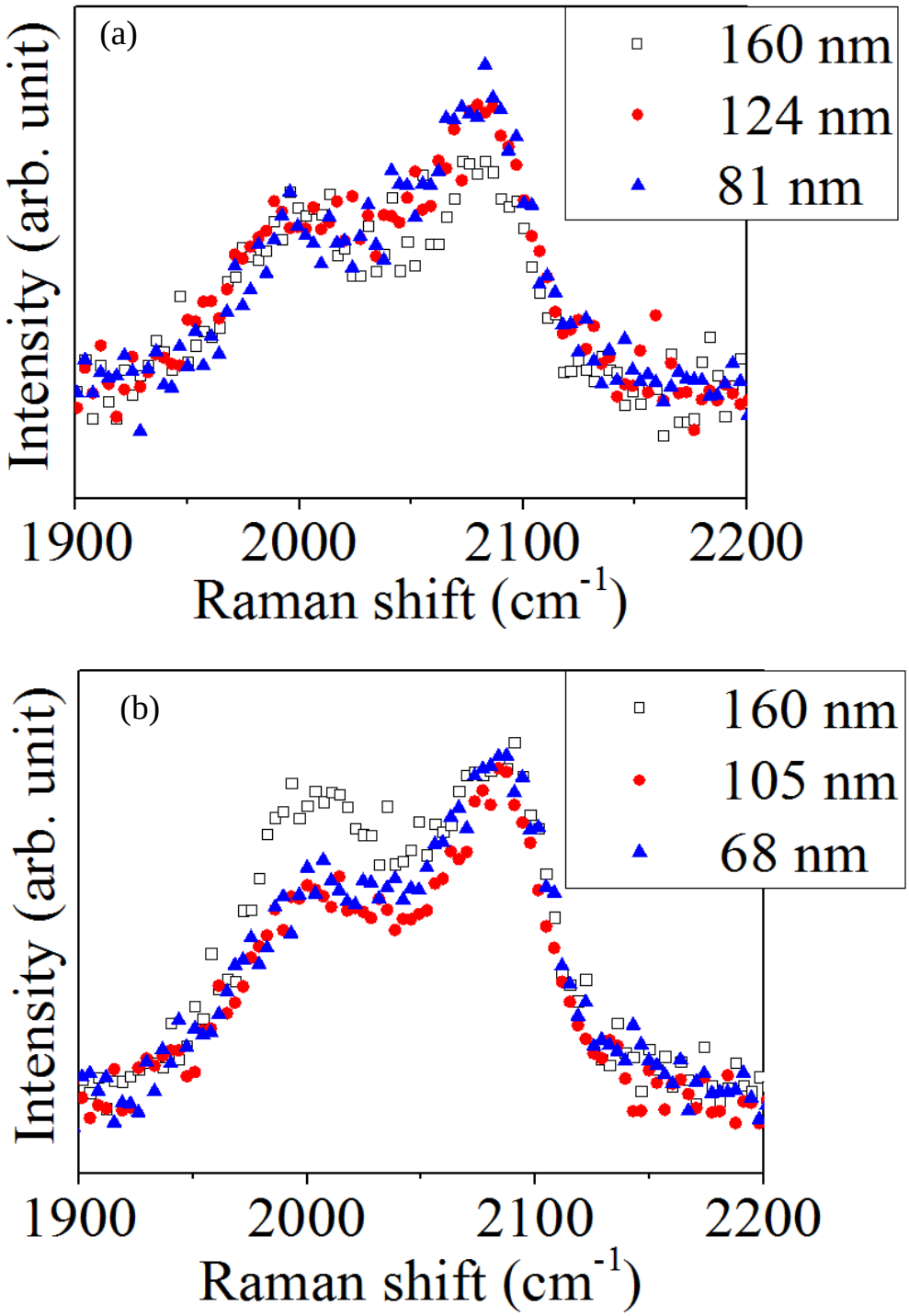
(a)
160 nm
124 nm
81 nm
Intensity (arb. unit)
1900
2000
2100
2200
Raman shift (cm-1)
(b)
160 nm
105 nm
68 nm
Intensity (arb. unit)
1900
2000
2100
2200
Raman shift (cm-1)